Songklanakarin J. Sci. Technol.
42 (2), 391-397, Mar. - Apr. 2020

http://www.sjst.psu.ac.th

Original Article

Hydrodynamic flow between rotating stretchable disks in an orthotropic porous medium

K. Gowthami[1], P. Hari Prasad[1], Bandaru Mallikarjuna[2*], and O. D. Makinde[3]

[1] *Department of Mathematics, Koneru Lakshmaiah Education Foundation, Vaddeswaram, Guntur, Andhra Pradesh, 522502 India*

[2] *Department of Mathematics, B. M. S. College of Engineering, Bangalore, Karnataka, 560019 India*

[3] *Faculty of Military Science, Stellenbosch University, Private Bag X2, Saldanha, 7395 South Africa*

Received: 22 June 2018; Revised: 13 November 2018; Accepted: 15 January 2019

Abstract

A mathematical model of convective steady flow over rotating disks in an orthotropic porous medium has been developed and solved the non-dimentional governing equations for flow by the shooting method that uses fourth order Runge- Kutta integration technique and Newton's method. Magnitude of radial velocity of fluid decreases near the surfaces of the disks for increasing value of Reynolds number. Impact of stretching parameters on the radial and tangential velocity profiles is observed. Computational results are presented graphically for various cases of parameters on velocity (radial f' and tangential g) and temperature profiles and table values are reported for skin friction and Nusselt number along both disks. It is observed that as the Reynolds number increases, the tangential velocity decreases. As we move far away from the disk the effects of physical parameters is not significant. It is seen that when the stretching parameter increases the radial velocity increases initially and when η=0.3 onwards the radial velocity decreases. This type of study finds application in industrial and engineering fields such as turbine engines and electronic power generating systems etc.

Keywords: rotating disks flow, porous medium, skin friction, heat transfer, shooting numerical method

1. Introduction

The steady flow of a viscous incompressible fluid between two rotatory stretchable disks is seen in many industrial, geothermal, geophysical, technological and engineering fields such as gas turbine engines, computer storage devices, electronic power generating systems, electronic devices which have rotatory parts, jet motors, turbine systems, air cleaning machines, plastic and metal industries, etc. With this motivation very interesting studies, both experimental and theoretical have been reported. Stewartson (1953) investigated both experimentally and theoretically the viscous fluid flow between two rotating disks. Lance and Rogers (1962) investigated the steady motion of symmetric flow of a viscous fluid between two rotating disks. Mellor, Chapple, and Stokes (1968) analysed the flow between two parallel disks by considering one in rotation and other at rest. Ramesh Chandra and Vijay Kumar (1972) investigated the heat transfer between two rotating disks by applying numerical method. Yan and Soong (1997) discussed numerically the influence of transpiration on the free and forced convection heat transfer flow between two parallel rotating disks.

*Corresponding author
Email address: mallikarjuna.jntua@gmail.com;
mallikarjunab.maths@bmsce.ac.in

Kishorekumar, William, and Layne (1989) examined numerically the magnetohydrodynamic (MHD) flow between two parallel disks by assuming one is in rotation and other at rest. Soong, Chang, Tung-Ping, and Tao-Ping (2003) have done a systematic study about the flow structure between two co-axial disks rotating independently. Fang and Zhang (2008) found an exact solution of the governing equations for the flow between two stretchable disks. Van Gorder, Sweet, and Vajravelu (2010) used an analytical method (HAM) to study the symmetric flow between two parallel stretchable disks. Latif and Peter (2010) studied heat transfer flow between two parallel rotating disks bifurcated by gas-filled micro-gap. Rashidi, Mohimanian, Hayat, and Obaidat (2012) used homotopy analysis method for the approximate solutions for steady flow over a rotating disk in porous medium with heat transfer. Rashidi, Ali, Freidoonimehr, and Nazar (2013) presented HAM solutions for the steady convective flow of a viscous incompressible fluid over a stretching rotating disk. Hatami, Sheikholeslami, and Ganji (2014) used least square method to find the solution of the problem on convection flow of a nano fluid between rotating disk and contracting rotating disks. Imtiaz, Hayat, Alsaedi, and Ahmed (2016) studied the thermal radiation effect on convective flow of carbon nanotubes between two parallel rotating stretchable disks. Hayat, Muhammad, Shehzad, and Alsaedi (2016) studied the slip effects on MHD heat transfer flow of nanofluid in between two rotating disks. Mallikarjuna, Rashidi, and Hariprasad Raju (2017) studied thermophoresis on double diffusive flow over a rotating cone with non-linear Boussinesq approximation. Mamatha, Raju, Saleem, Alderremy, and Mahesha (2018) investigated on MHD flow past a stretching cylinder filled nanoparticles using Cattaneo and Christov heat flux model. Raju, Saleem, Mamatha, and Hussain (2018) studied on double diffusive radiative flow past a slender body in porous media using Buongiorno's model.

Till now no one has studied the flow of rotating stretchable disks in an orthotropic porous medium. The authors aimed to investigate on convective flow between two rotating parallel stretchable disks. Therefore, our aim is to investigate heat transfer flow of a viscous fluid between two disks which are rotating with different angular velocity embedded in an orthotropic porous medium.

2. Problem Formulation

Consider two dimensional steady viscous incompressible flow between rotating disks as shown in Figure 1. The lower disk is placed at z=0 and upper disk is placed at z=d. The lower and upper disks are rotating with different constant angular velocities Ω_1 and Ω_2 respectively. Both the disks are assumed to be stretched in radial direction for various stretching rates b_1 and b_2 respectively. The lower and upper disks are maintained with different uniform constant temperature T_0 and T_1 respectively. The total system is embedded in an orthotropic porous medium. With the above assumption the governing equations in polar coordinates are as follows (Rashidi, Mohimanian, Hayat, & Obaidat 2012):

$$\frac{\partial U}{\partial r}+\frac{U}{r}+\frac{\partial W}{\partial z}=0, \tag{1}$$

$$U\frac{\partial U}{\partial r}+w\frac{\partial U}{\partial z}-\frac{V^2}{r}=\frac{-1}{\rho}\frac{\partial p}{\partial r}+\upsilon\left(\frac{\partial^2 U}{\partial r^2}+\frac{1}{r}\frac{\partial U}{\partial r}+\frac{\partial^2 U}{\partial z^2}-\frac{U}{r^2}\right)-\frac{\upsilon}{K_r}U, \tag{2}$$

$$U\frac{\partial V}{\partial r}+w\frac{\partial V}{\partial z}-\frac{UV}{r}=\upsilon\left(\frac{\partial^2 V}{\partial r^2}+\frac{1}{r}\frac{\partial V}{\partial r}+\frac{\partial^2 V}{\partial z^2}-\frac{V}{r^2}\right)-\frac{\upsilon}{K_\theta}V, \tag{3}$$

$$U\frac{\partial W}{\partial r}+w\frac{\partial W}{\partial z}=\frac{-1}{\rho}\frac{\partial p}{\partial z}+\upsilon\left(\frac{\partial^2 W}{\partial r^2}+\frac{1}{r}\frac{\partial W}{\partial r}+\frac{\partial^2 W}{\partial z^2}\right)-\frac{\upsilon}{K_z}W, \tag{4}$$

$$U\frac{\partial T}{\partial r}+w\frac{\partial T}{\partial z}=\alpha\left(\frac{\partial^2 T}{\partial r^2}+\frac{1}{r}\frac{\partial T}{\partial r}+\frac{\partial^2 T}{\partial z^2}\right), \tag{5}$$

Associated boundary conditions are

$$\begin{aligned} &U=rb_1, V=r\Omega_1, W=0, T=T_0 \text{ at } z=0\\ &U=rb_2, V=r\Omega_2, W=0, T=T_1 \text{ at } z=d \end{aligned} \tag{6}$$

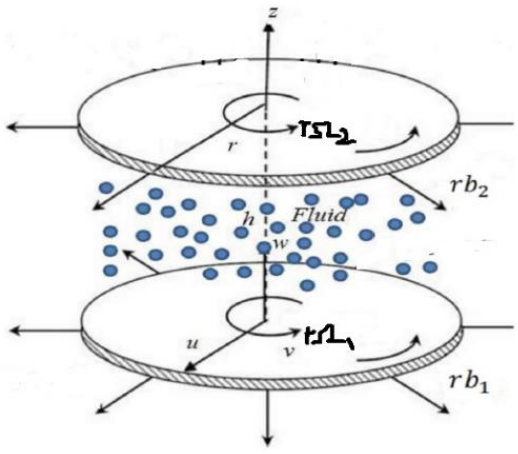

Figure 1. Geometry of the problem

Where U, V and W are velocity components in r,θ and z directions respectively, ρ is density, υ is the kinematic viscosity, K_r, K_θ and K_z are permeabilities in r,θ and z directions respectively and α is the thermal conductivity of fluid.

In order to non-dimensionalize the Equations (1) – (6), the following transformations are introduced

$$U = r\Omega_1 f'(\eta), V = r\Omega_1 g(\eta), W = -2\Omega_1 d f(\eta),$$
$$\eta = \frac{z}{d}, \Theta = \frac{T-T_1}{T_0-T_1}, p = \rho\Omega_1\upsilon\left(P(\eta) + \frac{r^2}{2d^2}\varepsilon\right) \quad (7)$$

Using (7), eqns. (1) – (6) become

$$f''' - \frac{1}{\mathrm{Re}}\left((f')^2 - 2ff'' - g^2\right) - \varepsilon - \frac{1}{k_1}f' = 0, \quad (8)$$

$$g'' - \frac{2}{\mathrm{Re}}\left(f'g - fg'\right) - \frac{1}{k_2}g = 0, \quad (9)$$

$$P' + \mathrm{Re}\, ff' + 2f'' - \frac{2}{k_3}f = 0, \quad (10)$$

$$\Theta'' + 2\,\mathrm{Re}\,\mathrm{Pr}\, f\Theta' = 0, \quad (11)$$

with the boundary conditions given as

$$f(0) = 0,\ f'(0) = R_1, g(0) = 1, \Theta(0) = 1$$
$$f(1) = 0,\ f'(1) = R_2, g(1) = \Omega, \Theta(1) = 0 \quad (12)$$

where $\mathrm{Re} = \frac{\Omega_1 d^2}{\upsilon}$ is the Reynold's number

$\mathrm{Pr} = \frac{\upsilon}{\alpha}$ is the Prandtl's number

$k_1 = \frac{K_r}{d^2}$ is the Darcy number along x-direction

$k_2 = \frac{K_\theta}{d^2}$ is the Darcy number along θ-direction

$k_3 = \frac{K_z}{d^2}$ is the Darcy number along z-direction

$\Omega = \frac{\Omega_2}{\Omega_1}$ is the rotation parameter

$R_1 = \frac{b_1}{\Omega_1}$, $R_2 = \frac{b_2}{\Omega_2}$ are scaled stretching parameters

The skin friction coefficients at the lower and upper disks are:

$$\tau_1 = \frac{\tau_w|_{z=0}}{\rho\left(r\Omega_1\right)^2} = \frac{\left(\left(f''(0)\right)^2 + \left(g'(0)\right)^2\right)^{1/2}}{\mathrm{Re}_r},$$
$$\tau_2 = \frac{\tau_w|_{z=h}}{\rho\left(r\Omega_2\right)^2} = \frac{\left(\left(f''(1)\right)^2 + \left(g'(1)\right)^2\right)^{1/2}}{\mathrm{Re}_r} \quad (13)$$

Rate of heat transfer (Nusselt numbers) at lower and upper disks are:

$$Nu_1 = \frac{-T_z|_{z=0}}{T_0 - T_1} = -\theta'(0)$$
$$Nu_2 = \frac{-T_z|_{z=h}}{T_0 - T_1} = -\theta'(1) \quad (14)$$

3. Numerical Procedure

A set of Equations (8) – (11) with conditions (12) are solved numerically, with the shooting method by Mallikarjuna, Rashad, Chamkha, and Hariprasad Raju (2016), Mallikarjuna, Rashad, Hussein, and Hariprasad Raju (2016), and Srinivasachary Mallikarjuna, and Bhuvanavijaya (2015) that uses Runge-Kutta method and Newton' method. To validate the present code the obtained results are compared with Stewartson (1953) and Imatiaz (2016) in the absence of heat transfer and porous media for limiting cases as shown in Table 1. The physical parameter values are assumed to be Re=10 (laminar flow), Pr =6.23 (light organic fluids), k_1=0.5, k_2 =0.5, R_1=0.7, R_2=0.7, Ω = 0.5 (see Mustafa (2016)) unless specified. Computational results are presented graphically for various cases of parameters on velocity (radial f' and tangential g) and temperature profiles and table values are reported for skin friction and Nusselt number along both disks.

4. Results and Discussion

Figure 2 illustrates the effect of k_1 on radial velocity. The parameter k_1 represents permeability along the radial direction. At the mean position of the disks the increase of the

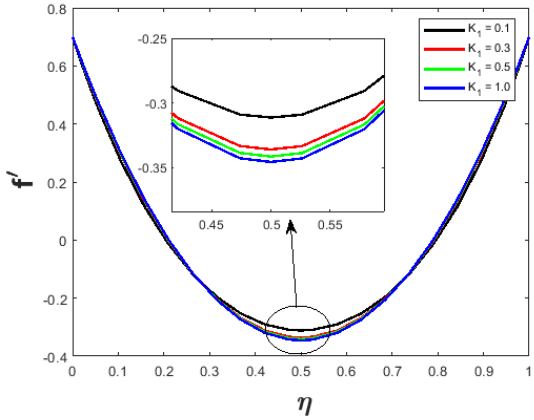

Figure 2. Effect of K_1 on f'

Table 1. Comparison of $f''(0)$ *and* $g'(0)$ for various values of Ω when R_1=0, R_2=0 and in the absence of porous medium for Re=1

Ω	K. Stewartson (1953)		Imtiaz, Hayat, Alsaedi, Ahmad (2016)		Present results	
	$f''(0)$	$-g'(0)$	$f''(0)$	$-g'(0)$	$f''(0)$	$-g'(0)$
-1	0.06666	2.00095	0.06666	2.00095	0.06666263	2.00095376
-0.3	0.10395	1.30442	0.10395	1.30442	0.10395043	1.30442628
0.5	0.06663	0.50261	0.06663	0.50261	0.06663394	0.50261755

permeability parameter results in deceleration of radial velocity and, moreover, the profiles are parabolic in nature. The effect of k_1 on the tangential velocity is shown in Figure 3. It is observed that permeability increases as the tangential velocity profiles increases. Figure 4 shows the effect of k_1 on temperature profiles. It is observed that when the permeability increases the temperature profile decreases. Enhancing permeability k_1 of the porous medium along the radial direction permits greater flow of the fluid in the tangential direction. Therefore, it decelerates the radial velocity and accelerates the tangential velocity and increases fluid temperature.

The effect of k_2 on radial velocity can be observed in Figure 5. At the mean position of a disk a permeability parameter increase results in an increase in the radial velocity and moreover, the profiles are parabolic in nature. Figure 6 illustrates the effect of k_2 on the tangential velocity; from the graph it is observed that as permeability increases the tangential velocity profile increases. Figure 7 shows the effect of k_2 on temperature profiles. It is observed that when permeability increases the temperature profiles decreases. Increasing Darcy number (enhancing permeability) k_2 of the porous medium along tangential direction permits greater flow of the fluid in the radial direction. Therefore, it accelerates the radial velocity and decelerates the tangential velocity and decreases fluid temperature.

Figure 8 illustrates the effect of R_1 on radial velocity. It is seen that when R_1 increases, the radial velocity increases initially and when η =0.3 onwards the radial velocity decreases. The effect of R_1on tangential velocity is observed in Figure 9. It is observed that as R_1 increases the tangential velocity profile decreases. Figure 10 shows the effect of R_1 on temperature profiles. It is observed that when R_1 increases the temperature profiles decreases. Increasing stretchable parameter R_1 at η=0 opposes the disk angular velocity and influences the adjacent fluid. Therefore, radical velocity is increased near the disk at η=0 and reversed at litter far to that disk.

The effect of R_2 on radial velocity is shown in Figure 11. It is observed that when R_2 increases radial velocity decreases and from η=0.7 the radial velocity increases. Figure 12 shows the effect of R_2 on tangential velocity. It is observed that when R_2 increases the tangential velocity increases. The effect of R_2 on temperature profile seen in Figure 13. It shows that as R_2 increases the temperature profiles increases. Increasing stretchable parameter R_2 at η=1 opposes the disk angular velocity and influences the adjacent fluid. Therefore, radical velocity increases near the disk at η=1 and is reversed from η=0 to a certain point.

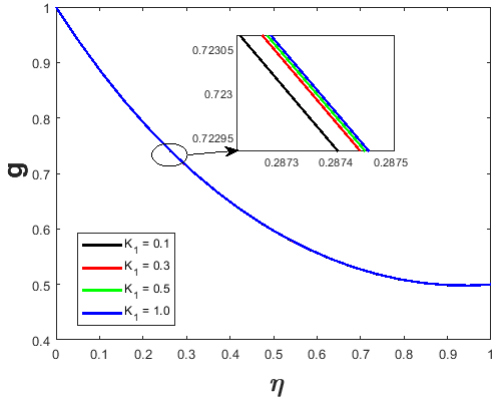

Figure 3. Effect of K_1 on g

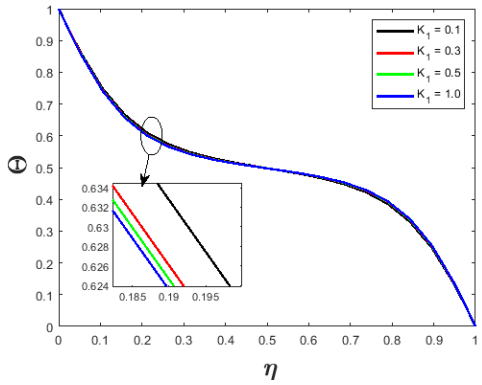

Figure 4. Effect of K_1 on temperature profiles

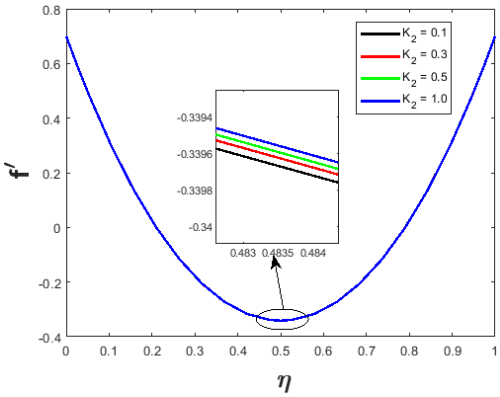

Figure 5. Effect of K_2 on f'

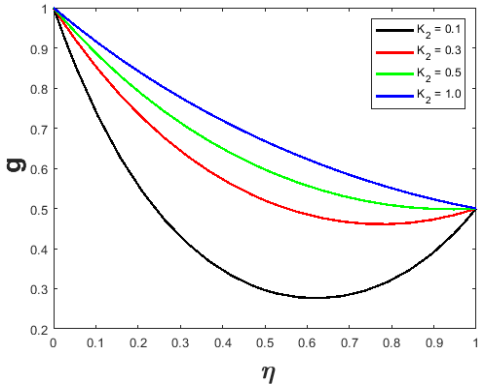

Figure 6. Effect of K_2on g

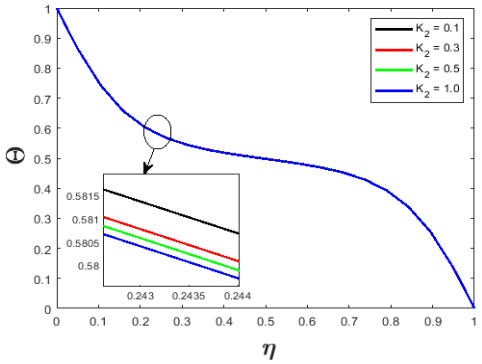

Figure 7. Effect of K_2 on temperature profiles

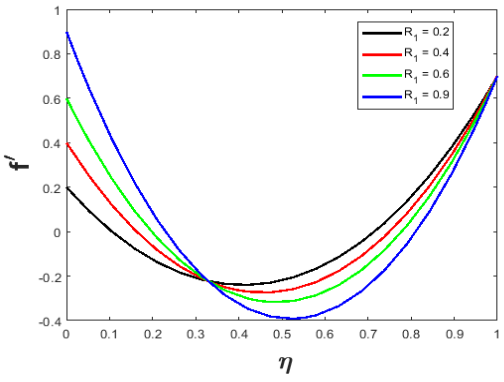

Figure 8. Effect of R_1 on f'

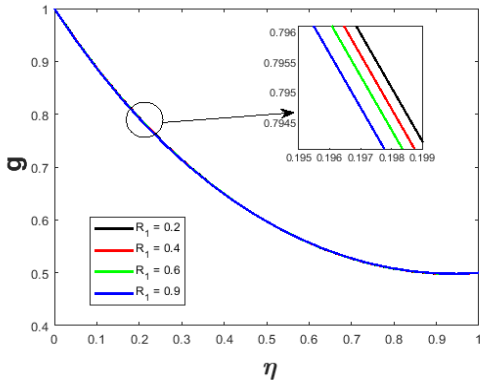

Figure 9. Effect of R_1 on g

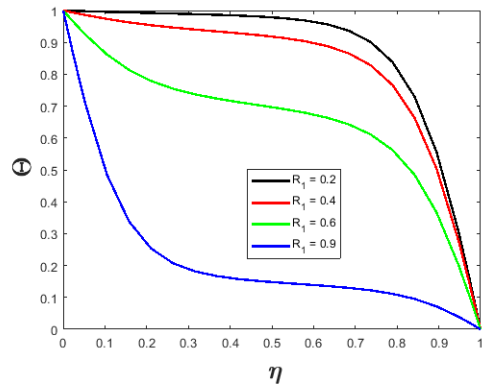

Figure 10. Effect of R_1 on temperature profiles

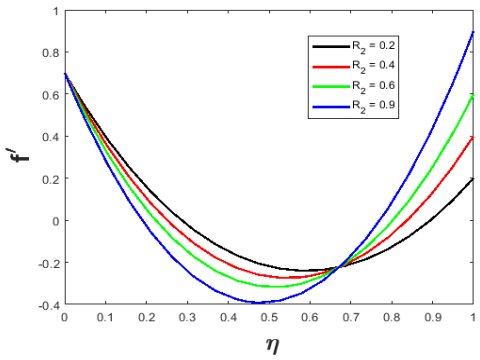

Figure 11. Effect of R_2 on f'

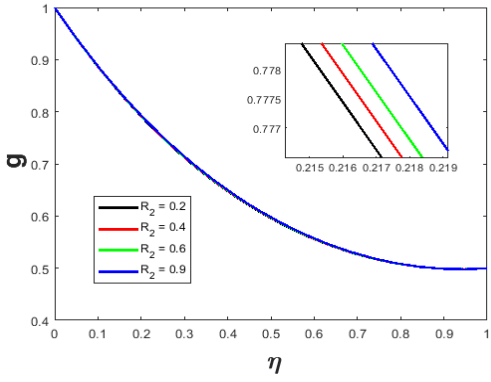

Figure 12. Effect of R_2 on g

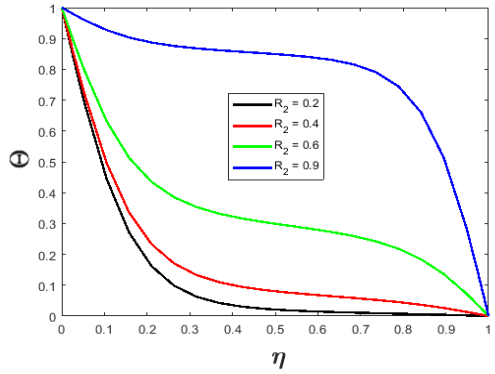

Figure 13. Effect of R_2 on temperature profiles

Table 2 shows the impact of Darcy numbers k_1, k_2, rotation parameter Ω, and scaled stretching parameters R_1, R_2 on skin friction coefficient at lower disk τ_1 and upper disk τ_2. It is observed that the skin friction coefficient at lower and upper disks decreases with the increasing values of k_1. When k_2 increases the values of τ_1 and τ_2 decrease. The skin friction coefficient at lower and upper disks decreases when the values of Ω increase. When R_1 increases the values of τ_1 and τ_2 increase. It is observed that when R_2values increase then τ_1 and τ_2 increase.

Table 2. Skin friction coefficient values at lower and upper disks Re=10, Pr=6.23.

K_1	K_2	Ω	R_1	R_2	τ_1	τ_2
0.1	0.5	0.5	0.7	0.7	5.00554926	4.86136052
0.3					4.59254700	4.43481529
0.5					4.50589128	4.34498479
	0.1				5.29967341	4.53883830
	0.3				4.62983393	4.35847810
	0.5				4.50589128	4.34498479
		0.2			4.56962298	4.36560446
		0.4			4.52594584	4.34616141
		0.8			4.45305449	4.37562491
		0.5	0.2		2.51467800	3.37922242
			0.4		3.28884477	3.76598075
			0.7		4.50589128	4.34498479
				0.2	3.58891528	2.20955789
				0.4	3.95334681	3.06299775
				0.6	4.32108445	3.91742165

From table 3 we observe that when k_1 increases the Nusselt number at the lower disk Nu_1 increases and the Nusselt number at the upper disk Nu_2 increases. With the increase of k_2, the Nusselt number at lower and upper disk increases. It also shows that the Nusselt number values at the lower disk decease and at the upper disk increase with the increase in the values of Ω. With the increased values of R_1 the Nusselt number values at the lower disk increase and at the upper disk decrease and with increased values R_2 the values of τ_1 decreases and τ_2 increase.

Table-3. Nusselt number values at lower and upper disks.

K_1	K_2	Ω	R_1	R_2	Nu_1	Nu_2
0.1	0.5	0.5	0.7	0.7	2.70517290	2.68136146
0.3					2.77295464	2.74507443
0.5					2.78744100	2.75858604
	0.1				2.78213929	2.76423857
	0.3				2.78614873	2.76002346
	0.5				2.78744100	2.75858604
		0.2			2.79150773	2.75457320
		0.4			2.78917483	2.75685730
		0.8			2.77997129	2.76612070
		0.5	0.2		0.04037686	6.03335654
			0.4		0.27202104	5.45796464
			0.7		2.78744100	2.75858604
				0.2	6.03965425	0.03958594
				0.4	5.47019476	0.26701219
				0.6	3.98882854	1.44860677

5. Conclusions

Heat transfer flow of viscous incompressible fluid between two parallel rotating disks with different angular velocity in an anisotropic porous medium has been investigated. Non-dimensionalized governing equations are solved numerically and the results are presented graphically on velocity (tangential and radial) and temperature profiles and table values are reported on skin friction and Nusselt number over two stretchable disks. The conclusions of the results are: with increasing Darcy numbers along x and θ – direction (k_1 and k_2) radial and tangential velocity profiles are increased and temperature profiles results show opposite behavior between the two stretchable disks. Increasing stretchable parameters (R_1 and R_2) results in velocity and temperature profiles with opposite behavior. The authors intend to extend this study with different boundary conditions and under thermal stratification.

References

Hatami, M., Sheikholeslami, M., & Ganji, D. D. (2014). Laminar flow and heat transfer of nanofluid between contracting and rotating disks by least square method. *Powder Technology, 253*, 769-779. doi:10.1016/j.powtec.2013.12.053

Hayat, T., Muhammad, T., Shehzad, S. A., & Alsaedi, A. (2016). On magnetohydrodynamic flow of nanofluid due to a rotating disk with slip effect: A numerical study. *Computer Methods in Applied Mechanics and Engineering*. doi:10.1016/j.cma.2016.11.002

Imtiaz, M., Hayat, T., Alsaedi, A., & Ahmad, B. (2016). Convective flow of carbon nanotubes between rotating stretchable disks with thermal radiation effects. *International Journal of Heat and Mass Transfer, 101*, 948-957. doi:10.1016/j.ijheatmasstransfer.2016.05.114

Kishorekumar, S., William, I. T., & Layne, T. W. (1989). Magneto hydrodynamic flow between a solid rotating disk and a porous stationary disk. *Physics of Fluid, 13*, 494-500. doi:10.1016/0307-904X(89)90098-X

Lance, G. N., & Rogers, M. H. (1962). The Axially symmetric flow of a viscous fluid between two infinite rotating disks. *Proceedings of the Royal Society a Mathematical Physical and Engineering Sciences 266*, 109-121. doi:10.1098/rspa.1962.0050

Latif, M. J., & Peter, G. (2010). Microscale flow and heat transfer between rotating disks. *International Journal of heat and fluid flow, 31*, 702–710. doi:10.1016/j.ijheatfluidflow.2010.02.008

Mallikarjuna, B., Rashad, A. M., Chamkha, A. J., & Hariprasad Raju, S. (2016). Chemical reaction effects on MHD convective heat and mass transfer flow past a rotating vertical cone embedded in a variable porosity regime. *Afrika Mathematika, 27*, 645-665. doi:10.1007/s13370-015-0372-1

Mallikarjuna, B., Rashad, A. M., Hussein, A. K., & Hariprasad Raju, S. (2016). Transpiration and thermophoresis effects on non-Darcy convective flow over a rotating cone with thermal radiation. *Arabian Journal for science and Engineering, 41*, 4691-4700. doi:10.1007/s13369-016-2252-x

Mallikarjuna, B., Rashidi, M. M., & Hariprasad Raju, S. (2017). Influence of nonlinear convection and thermophoresis on heat and mass transfer from a rotating cone to fluid flow in porous medium. *Thermal Science, 21*(6B), 2781-2793. doi:10.2298/TSCI150619004B

Mamatha, S. U., Raju, C. S. K., Saleem, S., Alderremy, A. A., & Mahesha. (2018). Modified Fourier heat flux on MHD flow over slender cylinder filled with dust, graphene and silver nanoparticles. *Results in Physics, 9*, 1377-1385. doi:10.1016/j.rinp.2018.04.038

Mellor, G. L, Chapple, P. J., & Stokes, V. K. (1968). On the flow between a rotating and a stationary disk. *Journal of Fluid Mechanics, 31*, 95-112. doi:10.1017/S0022112068000054

Ramesh Chandra, A., & Vijay Kumar, S. (1972). On the heat transfer between two rotating disks. *International Journal of Heat Mass Transfer, 15*, 2119-2132. doi:10.1016/0017-9310(72)90036-1

Mustafa, T. (2016). Flow and heat simultaneously induced by two stretchable rotating disks. *Physics of Fluids, 28*, 043601. doi:10.1063/1.4945651

Raju, C. S. K., Saleem, S., Mamatha, S. U., & Hussein, I. (2018). Heat and mass transport phenomena of radiated slender body of three revolutions with saturated porous: Buogiorno's model. *International Journal of Thermal Sciences, 132*, 309-315. doi:10.1016/j.ijthermalsci.2018.06.016

Rashidi, M. M., Mohimanian, S. A., Hayat, T., & Obaidat, S. (2012). Analytic approximate solutions for steady flow over a rotating disk in porous medium with heat transfer by homotopy analysis method. *Computers and Fluids, 54*, 1-9. doi:10.1016/j.compfluid.2011.08.001

Rashidi, M. M., Ali, M., Freidoonimehr, N., & Nazari, F. (2013). Parametric analysis and optimization of entropy generation in unsteady MHD flow over a stretching rotating disk using artificial neural network and particle swarm optimization algorithm. *Econ Papers, 55*, 497-510. doi:10.1016/j.energy.2013.01.036

Soong, C. Y., Chang-chie, W., Tung-Ping, L., & Tao–Ping, L. (2003). Flow structure between two co-axial disks rotating independently. *Experimental Thermal and Fluid Science, 27*, 295-311. doi:10.1007/s11630-003-0011-2

Srinivasacharya, D., Mallikarjuna, B., & Bhuvanavijaya, R. (2015). Soret and Dufour effects on mixed convection along a vertical wavy surface in a porous medium with variable properties. *Ain Shams Engineering Journal, 6*, 553-564. doi:10.1016/j.asej.2014.11.007

Stewartson, K. (1953). On the flow between two rotating coaxial disks. *Mathematical Proceedings of the Cambridge Philosophical Society 49*, 333-341. doi:10.1017/S0305004100028437

Tiegang, F., & Zhang, J. (2008). Flow between two stretchable disks – An exact solution of the Navier – Stokes Equations. *International Communications in Heat and Mass Transfer, 35*, 892-895. doi:10.1016/j.icheatmasstransfer.2008.04.018

Van Gorder, R. A., Sweet, E., & Vajravelu, K. (2010). Analytical solutions of a coupled non-linear system arising in a flow between stretching disks. *Applied Mathematics and Computation, 216*, 1513–1523. doi:10.1016/j.amc.2010.02.053

Yan, W. N., & Soong, C. Y. (1997). Mixed convection flow and heat transfer between two co-rotating porous disks with wall transpiration. *International Journal of Heat Mass Transfer, 40*, 773-784. doi:10.1016/0017-9310(96)00183-4